Growth of Snapdragon Under Simulated Transparent Photovoltaic Panels for Greenhouse Applications[1]

Eric J. Stallknecht[2], Christopher K. Herrera[3], Thomas D. Sharkey[4], Richard R. Lunt[3], and Erik S. Runkle[2]*

Abstract

Transparent photovoltaic (PV) materials can be used as greenhouse coverings that selectively transmit photosynthetically active radiation (PAR). Despite the economic importance of the floriculture industry, research on floriculture crops has been limited in these dual-purpose, agrivoltaic greenhouses. We grew snapdragon under simulated photoselective and neutral-density panels with transmissions ranging from ~30 to 90%, and absorption edges in the green (G; 500–599 nm), red (R; 600–699 nm), far-red (FR, 700–750 nm), and near-infrared (NIR) wavebands. We hypothesized that snapdragon could tolerate some degree of PV shading without reducing growth and flower number or delaying flowering time. Biomass accumulation, compactness, time to flower, and crop quality under 1) a clear acrylic control, 2) a FR-absorbing, and 3) a NIR-absorbing PV panel were not statistically different when the average daily light integral was between 17 and 20 mol·m^{-2}·d^{-1}. Crop quality progressively diminished below 17 mol·m^{-2}·d^{-1}. These results indicate that snapdragon tolerated ~15% PV shading during summer months without reduced growth or quality.

Species used in the study: Snapdragon (*Antirrhinum majus* L.).

Index words: Agrivoltaics, *Antirrhinum majus*, floriculture, greenhouse glazing.

Significance to the Horticulture Industry

An agrivoltaic greenhouse has the potential to synergistically co-localize energy and agricultural crop production. The development of transparent photovoltaics (PV) that selectively transmit photosynthetically active radiation could potentially be incorporated into greenhouse glazing materials with little to no effect on crop growth. The representative floriculture crop snapdragon grown under simulated semitransparent PV panels that absorbed far-red and near-infrared radiation had similar biomass accumulation, compactness, time to flower, and morphology compared to plants grown under a clear acrylic plastic during the summer. While agrivoltaic production is still early in development and has many unanswered questions, these promising results warrant further research on additional specialty crop types, at greenhouse locations, and especially on the economics of such a system before commercial greenhouse adoption.

Introduction

The current challenge to increase global food production and renewable energy sources paired with diminishing arable land requires reimagining contemporary agricultural production systems (Weselek et al. 2019). Incorporating photovoltaic (PV) panels into an agricultural system, often termed agrivoltaics, offers a unique opportunity to couple the production of agricultural crops and electrical generation to increase arable land-use efficiency (Amaducci et al. 2018, Dinesh and Pearce 2016, Proctor et al. 2020). However, crops and PV panels compete for a common resource: solar radiation. Consequently, a successful agrivoltaic system must prioritize crop yield and quality while also considering electrical generation. Furthermore, incorporating an agrivoltaic system into a greenhouse necessitates additional design considerations to account for year-round production. Therefore, a greenhouse-based agrivoltaic system must be designed using plant-centric principles to conserve crop yield and quality. For example, an agrivoltaic system must consider how PVs affect the greenhouse microclimate such as air temperature, canopy temperature, photosynthetic photon flux density (PPFD; 400–700 nm), transmission spectrum, and light uniformity, and how altered microclimate conditions influence crop yield and quality (Weselek et al. 2019).

Photovoltaic materials can range from opaque to semitransparent to visually transparent with controllable degrees of transmission (Traverse et al. 2017). The flexibility to control PV transmission is critical because greenhouse locations and the crops grown inside are extremely diverse. While opaque agrivoltaic materials are typically used for field installations, pilot studies in PV greenhouses have successfully used opaque to semitransparent materials covering roughly 10 to 30% of the greenhouse roof area to grow a diverse range of greenhouse crops including lettuce (*Lactuca sativa* L.), pepper (*Capsicum annuum* L.), tomato (*Solanum lycopersicum* L.), strawberry (*Fragaria* × *ananassa* Duch.), and petunia (*Petunia* × *hybrida* Hook.) without significantly decreasing crop yield or quality (Aroca-Delgado et al. 2019, Colantoni et al. 2018, Hassanien and Ming 2017, Kavga et al. 2019, Marrou et al. 2013, Tang et al. 2020, Toledo and Scognamiglio 2021). Opaque and semitransparent PVs most often function as shading materials that decrease the transmission of

Received for publication April 24, 2023; in revised form August 29, 2023.

[1]The authors thank the Horticultural Research Institute and the Michigan State University Climate Change Research Support Program Seed Grant for providing support of this work and Nathan DuRussel and Mckenna Merkel for technical support.

[2]Department of Horticulture, Michigan State University, East Lansing, MI, USA.

[3]Department of Chemical Engineering and Materials Science, Michigan State University, East Lansing, MI, USA.

[4]MSU-DOE Plant Research Laboratory and Department of Biochemistry and Molecular Biology, Michigan State University, East Lansing, MI, USA.

*Corresponding author: runkleer@msu.edu.

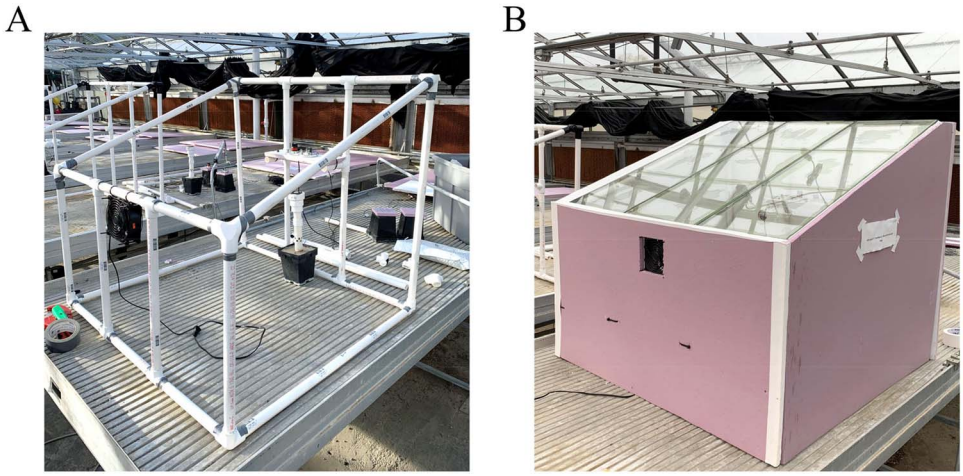

Fig. 1. Chambers covered with simulated semitransparent and transparent photovoltaic panels inside the Michigan State University research greenhouse facility. A) Chamber frames were constructed with polyvinyl chloride pipe. Each chamber was actively ventilated with a fan and equipped with an aspirated thermocouple and quantum sensors to continually measure air temperature and instantaneous photosynthetic photon flux density. B) Chamber walls were opaque to ensure light entering each chamber was transmitted through the experimental panels.

photosynthetically active radiation (PAR; 400–700 nm) or extended photosynthetically active radiation (ePAR; 400–750 nm) (Zhen and Bugbee 2020). Within a certain range, a 1% decrease in PAR transmission typically decreases crop yields by 0.75–1% (Marcelis et al. 2005). However, in high radiation environments, shading can decrease crop stress and increase the harvestable yield, partly by decreasing air temperature and increasing water-use efficiency (Barron-Gafford et al. 2019). In contrast, in lower radiation environments, permanent shading caused by PV installations could increase production time, decrease plant quality, or both, and necessitate supplemental lighting and more heating during the winter. To mitigate seasonal shading limitations, transparent PVs can be developed that transmit most of the incident (e)PAR, favorably modify transmission of the solar spectrum, or both.

Nearly all agrivoltaic research conducted in experimental PV-covered greenhouses has focused on growing leafy greens, culinary herbs, and fruiting crops such as lettuce, spinach (*Spinacia oleracea* L.), basil (*Ocimum basilicum* L.), tomato, and pepper. However, floriculture crops are a major segment of greenhouse crop production; it was valued at 6.4 and 50 billion USD in the U.S. and globally in 2021, respectively (USDA 2021). Leafy greens and many floriculture crops can be produced under a moderate average daily light integral (DLI; $mol \cdot m^{-2} \cdot d^{-1}$) whereas the harvestable yield of fruiting crops such as tomato usually decreases as the average DLI decreases (Cossu et al. 2020). Research focusing on floriculture crops produced inside a simulated agrivoltaic greenhouse is needed to quantify trade-offs that may exist between energy generation and crop timing and quality attributes. Here, we investigated the growth and flowering responses of snapdragon (*Antirrhinum majus* L.), which is a relatively commonly grown species of economic importance, and whose flowering response is influenced by day length, DLI, and the light spectrum. We hypothesized that snapdragon could tolerate some degree of PV shading with little to no decrease in growth or flower number, or delay in flowering time. We grew snapdragon under a range of experimental PV panels with different transmission spectra and quantified growth and flowering responses.

Materials and Methods

Chamber design. We constructed eight identical experimental chambers inside a glass-glazed research greenhouse at Michigan State University (42.7° N lat.) (Fig. 1A and B). Chambers were placed on aluminum benches (one per bench) that were positioned in a north-south orientation. Chamber frames were constructed of polyvinyl chloride (PVC) pipe and covered with an opaque, 1.9 cm (0.75 in) thick insulation board (FOAMULAR, Owens Corning, Toledo, OH). Each chamber provided ~0.90 m^2 (31.8 ft^3) of growing space and a volume of ~0.66 m^3 (23.3 ft^3). The interior insulation board surface was painted white to increase light scattering and uniformity. One electric 3.1 $m^3 \cdot min^{-1}$ (110 $ft^3 \cdot min^{-1}$) fan (Axial 1238, AC Infinity Inc., City of Industry, CA) was installed on the south-facing wall of each chamber, which was in the same wind direction as the greenhouse evaporative cooling system. Additionally, the north-facing wall was heavily perforated to increase air movement and prevent overheating. This mitigated the impact of air temperature on treatment effects. Each chamber roof was constructed from steel angle bars and supported various experimental PV panels. To increase light transmission and reduce cast shadows, chamber roofs were pitched 20 degrees south.

Simulated transparent PV panels. Simulated semitransparent and transparent PV panel transmission spectra are shown in Fig. 2A–C and were measured with a portable spectroradiometer at solar noon on a cloudless day (LI-180; LI-COR, Inc., Lincoln, NE). Table 1 quantifies the total photon flux density (TPFD; 400–750 nm) transmission divided into percent blue (B; 400–499 nm), green (G; 500–599 nm); red (R; 600–699 nm); and far-red (FR; 700–750 nm). Experimental panels included three neutral-density (ND) materials with 91, 58, and 33% transmission (henceforth termed clear plastic, moderate shade, and heavy

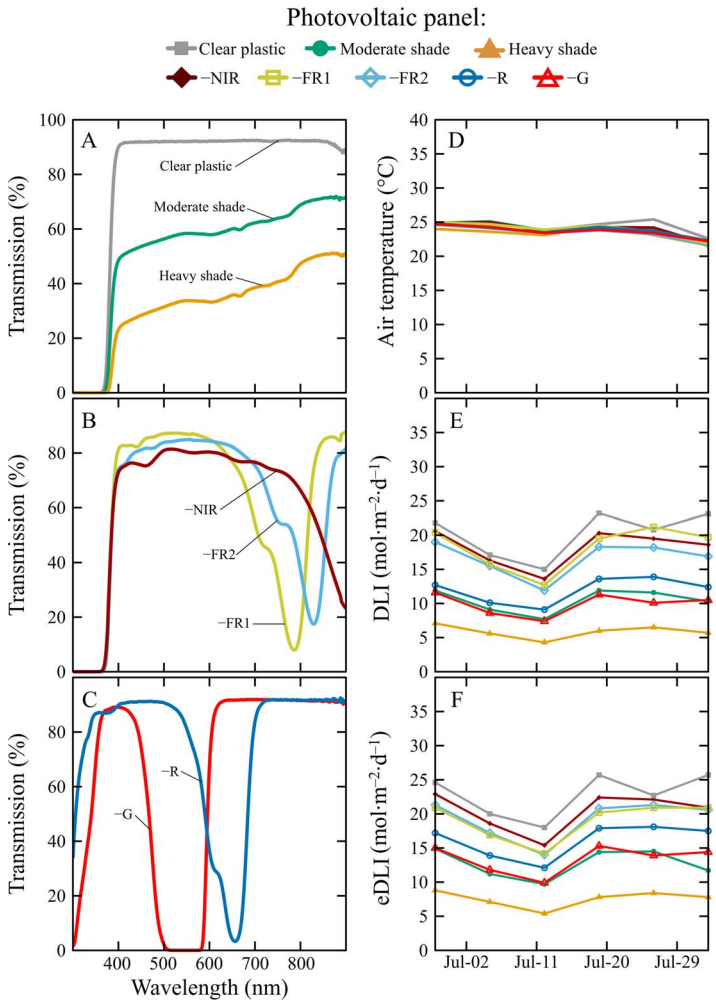

Fig. 2. **The transmission photon spectrum and average environmental conditions inside chambers covered with simulated semitransparent or transparent photovoltaic (PV) panels. A–C) Clear plastic, moderate shade, and heavy shade correspond to neutral-density materials with 91%, 58%, and 33% transmission from 400–700 nm. Near-infrared (NIR) deficient, far-red (FR; 700–800 nm) deficient 1 and 2, red (R; 600–700 nm) deficient, and green (G; 500–600 nm) deficient were simulated semitransparent or transparent PV panel with different transmission cutoffs between 400 and 850 nm. Transmission data were collected using a spectroradiometer. Transmissions were normalized to the incident photon flux density per nanometer of solar irradiance impinging on each chamber roof surface. Percentages of B, G, R, and FR light in each spectrum are displayed in Table 1. D–F) environmental conditions inside each chamber. Values represent weekly averages.**

shade, respectively) (Fig. 2A). ND materials did not meaningfully alter the transmitted solar spectrum. Additionally, five wavelength-selective panels were evaluated with cutoffs close to 475, 575, 700, 770, and 850 nm (henceforth termed −G, −R, −FR1, −FR2, and −NIR, respectively) (Fig. 2B and C). For example, the −G panel absorbed incident sunlight with a wavelength >475 nm and <600 nm to remove most of the G light.

Table 1. **The spectral characteristics of simulated semitransparent and transparent photovoltaic (PV) panels. Total photon flux density (TPFD; 400–750 nm) transmission was divided into percentages of blue (B; 400–499 nm), green (G; 500–599 nm); red (R; 600–699 nm); and far-red (FR; 700–750 nm) light. Phytochrome photoequilibrium (PPE) and internal phytochrome photoequilibrium (iPPE) were calculated according to Seger (1982) and Kusuma and Bugbee (2021), respectively. Clear plastic, moderate shade, and heavy shade correspond to neutral-density materials with 91%, 58%, and 33% transmission from 400–750 nm. Near-infrared (NIR) deficient, FR deficient 1 and 2, R deficient, and G deficient refer to experimental materials with different transmission cutoffs. Semitransparent and transparent PV panels are organized in descending order according to average (e)DLI from right to left.**

	Semitransparent and transparent photovoltaic panels							
Spectral characteristics	**Clear plastic**	**−NIR**	**−FR1**	**−FR2**	**−R**	**Moderate shade**	**−G**	**Heavy shade**
B (% of TPFD)	28.4	27.9	31.3	28.6	37.9	26.2	30.0	24.0
G (% of TPFD)	28.5	29.5	32.3	30.2	31.7	28.5	0.02	28.4
R (% of TPFD)	28.6	28.6	27.9	29.1	11.1	29.4	44.5	30.3
FR (% of TPFD)	14.6	14.0	0.09	12.0	19.2	15.8	23.2	17.2
PPE	0.70	0.71	0.76	0.73	0.56	0.69	0.70	0.69
iPPE	0.38	0.39	0.52	0.44	0.25	0.37	0.36	0.35

Preparation of wavelength-selective panels. (−G, −R, −FR1, −FR2, and −NIR): 3-Ethyl-2-[3-[3-ethyl-3H-benzothiazol-2-ylidene]-1-propenyl]-benzothiazolium iodide (Cy3-I, American Dye Source, Baie d'Urfé, Quebec, Canada), 2-[5-(1,3-Dihydro-3,3-dimethyl-1-propyl-2H-indol-2-ylidene)-1,3-pentadienyl]-3,3-dimethyl-1-propyl-3H-indolium perchlorate (Cy5-ClO_4, American Dye Source), 2-[2-[2-Chloro-3-[(1,3-dihydro-1,3,3-trimethyl-2H-indol-2-ylidene)ethylidene]-1-cylcohexen-1-yl]-ethenyl]-1,3,3-trimethyl-1H-indolium iodide (IR775-I, Few Chemicals, Bitterfeld-Wolfen, Germany), 2-[2-[2-chloro-3-[2-(1,3-dihydro-3,3-dimethyl-1-ethyl-2H-benz[e]indol-2-ylidene)ethylidene]-1-cylohexen-1-yl]-ethenyl]-3,3-dimethyl-1-ethyl-1H-benz[e]indolium iodide (Cy-I, American Dye Source), 1-Butyl-2-(2-[3-[2-(1-butyl-1H-benzo[cd]idnol-2-ylidene)-ethylidene]-2-diphenylamino-cyclopent-1-enyl]-vinyl)-benzo[cd]indolium tetrafluoroborate (IR996-BF_4, Few Chemicals). Cy3-I, Cy5-ClO_4, IR775-Cl, Cy-I, and IR996-BF_4 were mixed with potassium tetrakis(pentafluorophenyl) borate (K-TPFB) as described by Suddard-Bangsund et al. (2016) to create Cy3-TPFB (−G), Cy5-TPFB (−R), IR775-TPFB (−FR1), Cy-TPFB (−FR2), and IR996-TPFB (−NIR). −G, −R, −FR1, −FR2, and −NIR were cast into a solid film using a Shandon mounting media (CAS#9990435, Thermo Fisher Scientific, Waltham, MA) and sealed in a nitrogen environment as previously described in Stallknecht et al. (2023).

Environmental sensing. Each chamber was equipped with an aspirated thermocouple (Type E; Omega Engineering, Inc., Stamford, CT) to measure air temperature. Additionally, each chamber had a quantum sensor (400–700 nm) (LI-190SA; LI-COR, Inc., or SQ-500; Apogee Instruments, Inc., Logan, UT) and ePAR quantum sensor (400–750 nm) (SQ-610; Apogee Instruments, Inc.) to measure instantaneous PPFD and TPFD at the top of the crop canopy, respectively. Thermocouples and quantum sensors were connected to a CR1000 datalogger (Campbell Scientific, Logan, UT) and AM16/32B multiplexer (Campbell Scientific) combination that sampled environmental conditions every minute and recorded hourly averages. Instantaneous PPFD and TPFD measurements were integrated daily to calculate the DLI and eDLI. Average chamber air temperature, DLI, and eDLI are depicted in Fig. 2D–F.

Greenhouse environment. The greenhouse environment was regulated by an Integro 725 (Priva North America, Vineland Station, ON, Canada) control system. The air temperature setpoint was a constant 21 C (70 F). Heating was provided by radiant steam and cooling was provided through roof vents, exhaust fans, and an evaporative cooling pad.

Snapdragon seedling growth. Snapdragon 'Snapshoot Yellow' (PanAmerican Seed Co., West Chicago, IL) seeds were sown on 2 June 2021 into 288-cell (8-mL individual cell volume) plug trays filled with a peat-based soilless substrate composed of 70% peat moss, 21% perlite, and 9% vermiculite (Suremix; Michigan Grower Products, Inc., Galesburg, MI). Plug trays were placed into a controlled-environment growth room at 21 C (70 F) air temperature, 9-h photoperiod, and a PPFD of 180 $\mu mol \cdot m^{-2} \cdot s^{-1}$ at canopy height (DLI = 5.8 $mol \cdot m^{-2} \cdot d^{-1}$). The light was provided by white, blue, and red light-emitting diodes (RAY 44 Physiospec Indoor; Fluence Bioengineering; Austin, TX). Plug trays were covered for one week with transparent humidity domes. Seedlings were irrigated as needed with a solution of deionized water, hydroponic water-soluble fertilizer (12N–1.7P–13.3K RO Hydro FeED, JR Peters, Inc, Allentown, PA), and magnesium sulfate (Epsom salt, Pennington Seed Inc., Madison GA). This provided the following nutrients (in mg L^{-1}): 125 N, 18 P, 138 K, 73 Ca, 49 Mg, 37 S, 1.6 Fe, 0.5 Mn, 0.4 Zn, 0.2 B and Cu, and 0.01 Mo. The fertilizer solution was adjusted to a pH of 5.8 and electrical conductivity of 1.2 $mS \cdot cm^{-1}$ with a handheld meter (HI9814; Hanna Instruments, Woonsocket, RI) upon formulation.

Snapdragon mature growth. Snapdragon seedlings were transplanted on 28 June 2021 into 10-cm (4-in) pots filled with the same peat-based potting media used to grow seedlings. Plants were irrigated as needed with a solution consisting of reverse osmosis water supplemented with 13N–1.3P–12.5K water-soluble fertilizer that contained (in $mg \cdot L^{-1}$) 125 N, 13 P, 120 K, 77 Ca, 19 Mg, 1.7 Fe, 0.4 Cu, and Zn, 0.8 Mn, 0.2 B and Mo (MSU Orchid RO Water Special; GreenCare Fertilizers, Inc., Kankakee, IL).

Experimental design and statistics. The experiment was organized as a completely randomized design where 15 uniform snapdragon seedlings were randomly transplanted into one of eight chambers (experimental unit) that had one randomly assigned experimental PV treatment. The experiment was replicated once. Data were analyzed in R software (Version 4.2.2, The R Foundation, Vienna, Austria) using analysis of variance (ANOVA) and Tukey's honestly significant difference test at $\alpha = 0.05$ (n=15).

Data collection. Snapdragon grew under natural photoperiods for 36 days (after transplant) until destructive measurements were taken on 23 August 2021. Time to first visible bud (VB) was recorded when a flower bud was visible with the naked eye on the terminal inflorescence, and time to first open flower was recorded when the first flower of the terminal inflorescent fully opened. At harvest, central stem length and diameter were measured with a ruler and digital calipers (41101 DigiMax; Wiha Switzerland, Monticello, MN, USA). The total number of flowers, flowers on the terminal inflorescence, and nodes under the terminal inflorescence were counted. For each plant, the length, width, and relative chlorophyll content was measured on three leaves with a ruler and SPAD meter (MC-100; Apogee Instruments, Inc., Logan, UT) and averaged for each sample. Specific leaf area (SLA; $cm^2 \cdot g^{-1}$) was calculated by dividing the leaf area of the three representative leaves [measured by a leaf area meter (LI-3100 Area Meter; LI-COR, Inc.)] by their dry mass and averaged per sample. Shoot fresh mass was measured with a digital scale at the time of harvest (GR-200; A&D Store, Inc., Wood Dale, IL). Shoot dry mass after four days in a 60 C (140 F) drying oven (SMO28-2; Sheldon Manufacturing, Inc., Cornelius, OR) was measured with a digital scale (GX-1000; A&D Store, Inc.). Radiation-use efficiency

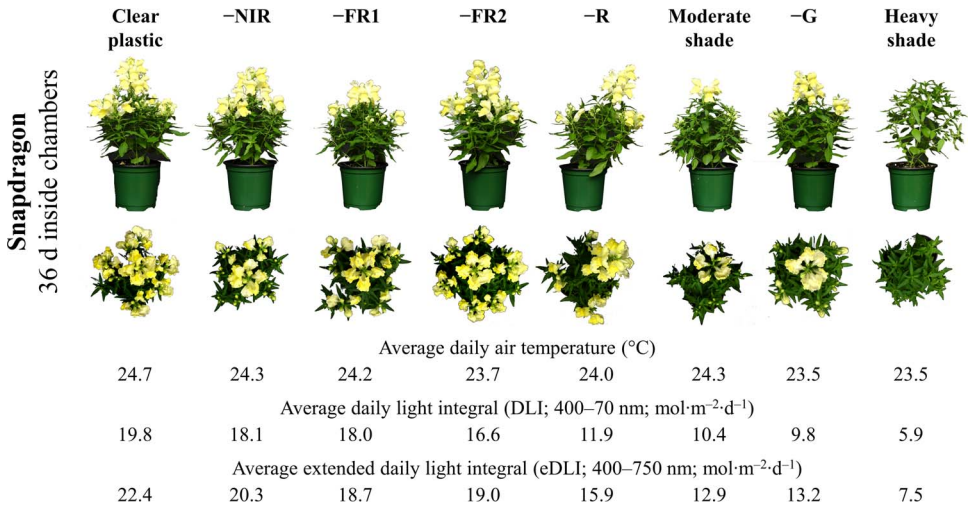

Fig. 3. Photographs of representative snapdragon plants grown under eight different simulated semitransparent and transparent photovoltaic (PV) panels. Semitransparent and transparent PV panel spectra are displayed in Table 1 and Fig. 2A–C. Average daily air temperature (C), daily light integral (DLI; 400–700 nm), and extended daily light integral (eDLI; 400–750 nm) were measured at canopy height. Values represent daily means and are organized in descending order according to (e)DLI from right to left.

(RUE; g shoot dry mass·mol^{-1} photon) was calculated by dividing shoot dry mass by the accumulated DLI (mol·m^{-2}) while snapdragon plants were in the chambers. The sturdiness quotient (SQ; cm·mm^{-1}) was calculated by dividing stem length by stem diameter (Jaenicke 1999).

Results and Discussion

Chamber environmental conditions. Average chamber air temperature, DLI, and eDLI are reported in Fig. 2D–F and Fig. 3. Average daily air temperature deviated by a maximum of 1.2 C (2.2 F) between treatments, and the largest deviation occurred between the clear-plastic and heavy-shade treatments. Air temperature variations between treatments were not correlated with DLI or eDLI (P=0.056 and P=0.058, respectively) and were likely caused by minor micro-climates within the research greenhouse. Similar to air temperature, the average DLI and eDLI were greatest under the clear-plastic treatment and lowest under the heavy-shade treatment. The DLI and eDLI were significantly correlated between treatments (P<0.001; r^2=0.96).

Biomass accumulation. Snapdragon shoot dry mass (SDM) was greatest under treatments with the highest light transmission (clear plastic, −NIR, −FR1, and −FR2) and lowest under the heavy-shade treatment Fig. 4A; Table 2). Snapdragon SDM was positively correlated to treatment DLI and eDLI (Fig. 4A; Table 3 and 4) and decreased by ∼65% when transmission decreased by ∼67% (i.e., 67% shade). At a similar average DLI (∼11 mol·m^{-2}·d^{-1}), snapdragon SDM was greater under the −G and −R treatments than under the moderate-shade treatment that had no spectral manipulation between 400 and 700 nm. These results indicate that PV panel transmission and spectrum both influenced snapdragon biomass accumulation.

Radiation-use efficiency (RUE) is the ratio of accumulated dry mass to the total quantity of light intercepted by a plant (g SDM per mol PAR intercepted) and is a common plant performance metric for light utilization. Critical to agrivoltaic research, RUE is sensitive to light spectrum and PPFD (Jayalath and van Iersel 2021, Ke et al. 2022, Wollaeger and Runkle 2014). Snapdragon RUE was greatest in the moderate- and heavy-shade treatments and ∼55% greater than snapdragon under the clear-plastic treatment (Table 2). As DLI and eDLI increased, snapdragon RUE decreased linearly (Table 3, 4). Snapdragon grown during the summer under PV panels tolerated approximately a 15% decrease in DLI and eDLI transmission without significantly affecting snapdragon biomass accumulation.

Snapdragon biomass accumulation under a range of potential PV panel transmissions was consistent with the paradigm that a 1% decrease in light equates to ∼0.75 to 1% decrease in SDM (Marcelis et al. 2005) when the average DLI decreased from 19.8 to 5.9 mol·m^{-2}·d^{-1}. However, snapdragon SDM was similar when the DLI decreased by 16% from 19.8 to 16.6 mol·m^{-2}·d^{-1}. In a separate study, SDM decreased by 64% as the DLI decreased from 21.8 to 10.5 mol·m^{-2}·d^{-1} (by 52%) but decreasing the DLI from 21.8 to 17.8 (18%) produced snapdragon with a similar SDM (Warner and Erwin 2005). This decrease in SDW of snapdragon with a decrease in DLI is consistent between studies as well as other common floriculture crops including impatiens (*Impatiens wallerana* Hook.), cyclamen (*Cyclamen persicum* Mill.), and periwinkle (*Catharanthus roseus* L.) (Faust et al. 2005, Oh et al. 2009, Warner and Erwin 2005). In addition, biomass accumulation of petunia under transparent PV tolerated ∼20–25% PV shading during summer months without decreasing SDM (Stallknecht et al. 2023). Thus, decreasing (e)DLI by 15–25% (beyond that of traditional glazing materials) is likely an acceptable shading factor for most floriculture crops grown during high-light periods, e.g., April through August in the northern hemisphere. Because snapdragon and petunia grown under experimental transparent

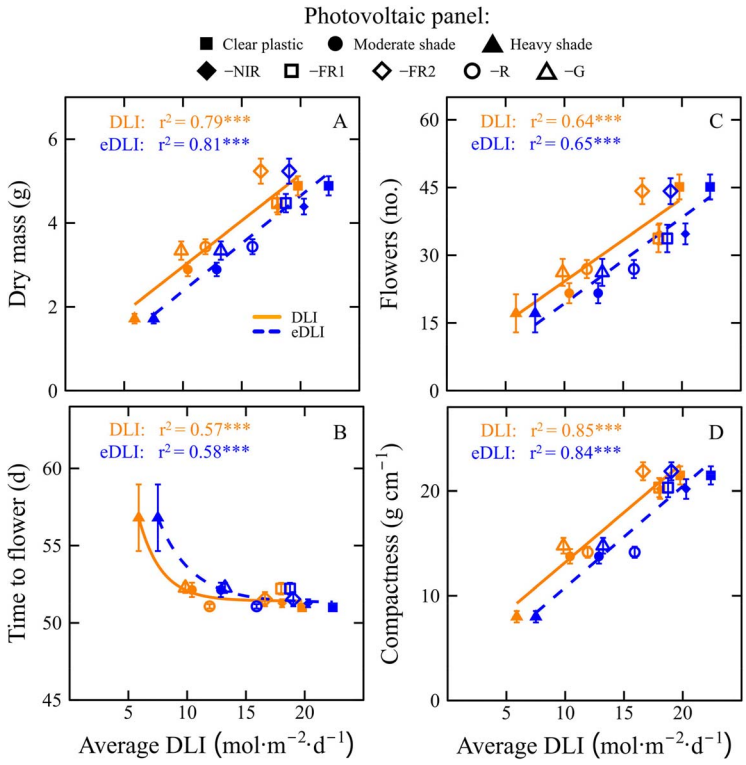

Fig. 4. Key growth metrics for snapdragon grown under eight different simulated semitransparent and transparent photovoltaic (PV) panels as a function of daily light integral (DLI; 400–700 nm) and extended daily light integral (eDLI; 400–750 nm). Simulated semitransparent and transparent PV panel transmission spectra are displayed in Table 1 and Fig. 2A–C. Average DLI and eDLI were measured at canopy height. Time to flower was calculated from seed sow to first open floret. Flower number integrated all open florets and visible buds. Compactness was calculated according to table 2. Regression equations are displayed in Tables 3 and 4. Values represent averages ± 95% CI (n=15). Asterisks indicate significance at $P < 0.05$, $P < 0.01$, and $P < 0.001$ and are designated by *, **, and *, respectively. Regression equations are displayed in Tables 3 and 4.**

PV panels follow the paradigm regarding biomass accumulation and light quantity, the effects of experimental PV panels on floriculture crop production can be predicted based on DLI responses already published.

Growing ornamental greenhouse crops only during high-light periods does not fully describe long-term shading effects on crop production during light-limited periods. A typical greenhouse glazing material has a solar transmission of ~70–90% and a greenhouse macro-structure can further reduce the amount of light reaching crops by an additional ~20–35% (Both 2002, Giacomelli and Roberts 1993). In sum, the average transmission of (e)PAR incident upon a greenhouse crop can range from 40–70% of that outdoors (Von Elsner et al. 2000). In the current work,

Table 2. Growth of snapdragon under eight different simulated semitransparent and transparent photovoltaic (PV) panels. Time to visible bud (VB) was calculated from seed sow. Radiation-use efficiency (RUE) was calculated by dividing total dry biomass accumulation (g) by accumulated daily light integral (mol photon·m^{-2}; 400–700 nm) while snapdragon was inside the experimental chambers. Specific leaf area (SLA) was calculated by dividing leaf area (cm^2) by leaf mass (g) of three representative leaves per plant. Compactness was calculated by dividing the total above-ground dry mass (g) by stem length (cm). The sturdiness quotient (SQ) was calculated by dividing stem length (cm) by the stem diameter at the substrate surface (mm). Data represent means with 15 samples. Means with different letters are significantly different according to Tukey's honestly significant difference test ($P < 0.05$) and correspond to each row. Semitransparent and transparent PV panels are organized in descending order according to average (e)DLI from right to left.

	Semitransparent and transparent photovoltaic panels							
Growth parameter	**Clear plastic**	**−NIR**	**−FR1**	**−FR2**	**−R**	**Moderate shade**	**−G**	**Heavy shade**
Fresh mass (g)	35.5 b	32.4 c	34.7 bc	40.7 a	26.9 d	23.1 e	26.2 d	14.7 f
RUE (g·mol^{-1})	0.29 c	0.33 c	0.31 c	0.33 c	0.38 b	0.42 ab	0.40 b	0.47 a
Time to VB (d)	40 c	40 bc	40 b	40 c	40 bc	40 bc	40 bc	42 a
Leaf length (cm)	5.25 bc	5.05 c	5.56 ab	5.68 a	5.41 abc	5.23 bc	5.35 abc	5.11 c
Leaf width (cm)	1.81 ab	1.55 d	1.77 abc	1.93 a	1.75 abcd	1.57 cd	1.67 bcd	1.75 abcd
SPAD	30.9 ab	31.7 a	32.0 a	29.8 ab	26.7 d	29.3 bc	26.3 d	27.2 cd
SLA (cm^2·g^{-1})	510 e	499 e	542 de	555 cde	609 b	598 cd	659 bc	743 a
Stem length (cm)	23.0 ab	22.0 b	22.2 b	24.1 a	24.4 a	21.2 b	22.8 ab	21.8 b
Stem diameter (mm)	4.15 b	4.18 b	4.64 a	4.71 a	3.39 d	3.98 b	3.83 bc	3.49 cd
SQ (cm·mm^{-1})	5.42 cd	5.28 d	4.79 d	5.16 d	7.24 a	5.41 cd	5.96 bc	6.33 b

Table 3. Regression coefficients for snapdragon growth parameters as a function of average daily light integral (DLI; 400–700 nm; mol·m^{-2}·d^{-1}). Radiation-use efficiency (RUE), time to visible flower bud (VB), specific leaf area (SLA), compactness, and sturdiness quotient (SQ) calculations are defined in Table 2. Linear, quadratic, and sigmoidal functions were evaluated as possible regression types. The regression with the highest r^2 value was selected, unless not meaningfully better than a linear model. In this case, a linear model was selected. Asterisks indicate significance at $P < 0.05$, $P < 0.01$, and $P < 0.001$ and are designated by *, **, and *, respectively. N.S. = not significant. n=120.**

Growth parameter	Regression type	Equation	
Fresh mass (g)	Sigmoidal	$y = 39.3 * \exp(-2.97 * 0.831^X)$	$r^2 = 0.77$***
Dry mass (g)	Linear	$y = 0.220 * x + 0.765$	$r^2 = 0.79$***
RUE (g·mol^{-1})	Linear	$y = -0.0115 * x + 0.525$	$r^2 = 0.66$***
Time to VB (d)	Sigmoidal	$y = 39.8 * \exp(0.914 * 0.616^X)$	$r^2 = 0.53$***
Time to flower (d)	Sigmoidal	$y = 51.4 * \exp(1.88 * 0.607^X)$	$r^2 = 0.57$***
Flowers (no.)	Linear	$y = 1.85 * x + 5.59$	$r^2 = 0.64$***
Leaf length (cm)	-	-	N.S.
Leaf width (cm)	-	-	N.S.
SPAD	Linear	$y = 0.376 * x + 24.0$	$r^2 = 0.38$***
SLA (cm^2·g^{-1})	Linear	$y = -15.7 * x + 806$	$r^2 = 0.64$
Stem length (cm)	Quadratic	$y = (-0.0290 * x^2) + (0.790 * x) + 17.8$	$r^2 = 0.08$**
Stem diameter (mm)	Linear	$y = 0.0707 * x + 3.07$	$r^2 = 0.33$***
Compactness (g·m^{-1})	Linear	$y = 0.951 * x + 3.68$	$r^2 = 0.85$***
SQ (cm·mm^{-1})	Linear	$y = -0.0970 * x + 7.04$	$r^2 = 0.22$***

the highest light transmission panels (−NIR, −FR1, and −FR2) were similar to those of conventional greenhouse glazing materials (~75-80%) such as twin-wall polycarbonate or double-layer polyethylene (Both 2002, Giacomelli and Roberts 1993). Even with a high-transmission glazing material and minimal overhead obstructions, supplemental lighting is sometimes used from early winter to mid-spring, which is when most annual bedding plants are produced. While PV panels that absorb (e)PAR would increase electricity generation, decreasing PAR transmission would come at the expense of crop quality and production time. Therefore, in temperate climates, transparent PV panels that maximize the transmission of PAR (yet absorb UV and NIR for electricity generation) are needed for year-round agrivoltaic greenhouse crop production.

The tolerance to light transmission decreases by PV panels depends on the greenhouse location and crops grown. For instance, the DLI outside in January typically ranges from 5–10 mol·m^{-2}·d^{-1} in Michigan but 20–25 mol·m^{-2}·d^{-1} in Arizona (Faust and Logan 2018). Consequently, transparent PV panels have greater energy generation potential in high-light areas, as well as a greater opportunity to manipulate the light spectrum to elicit desirable morphological changes. At a similar light intensity, crops grown under a light spectrum with a greater fraction of R and FR photons generally have a higher RUE from increased extension growth (e.g., leaf surface area or stem elongation) and light interception (Jayalath and van Iersel 2021, Ke et al. 2022, Meng et al. 2019, Meng et al. 2020, Wollaeger and Runkle 2014,). Thus, PV panels that target the absorption of B or G light, in addition to UV and NIR, could increase the biomass accumulation and RUE of some greenhouse crops grown in high-light regions if changes to plant morphology are tolerable.

Flowering. Time to first visible inflorescence and open flower were similar among most treatments except for the heavy-shade treatment, which occurred 2 or 5 d later (Fig. 4B). Thus, the flowering of snapdragon was delayed when

Table 4. Regression coefficients for snapdragon growth parameters as a function of average extended daily light integral (eDLI; 400–750 nm; mol·m^{-2}·d^{-1}). Radiation-use efficiency (RUE), time to visible flower bud (VB), specific leaf area (SLA), compactness, and sturdiness quotient (SQ) calculations are defined in Table 2. Linear, quadratic, and sigmoidal functions were evaluated as possible regression types. The regression with the highest r^2 value was selected, unless not meaningfully better than a linear model. In this case, a linear model was selected. Asterisks indicate significance at $P < 0.05$, $P < 0.01$, and $P < 0.001$ and are designated by *, **, and *, respectively. N.S. = not significant. n=120.**

Growth parameter	Regression type	Equation	
Fresh mass (g)	Sigmoidal	$y = 44.2 * \exp(-2.93 * 0.881^X)$	$r^2 = 0.76$***
Dry mass (g)	Linear	$y = 0.227 * x + 0.105$	$r^2 = 0.81$***
RUE (g·mol^{-1})	Linear	$y = -0.0115 * x + 0.554$	$r^2 = 0.64$***
Time to VB (d)	Sigmoidal	$y = 39.7 * \exp(0.557 * 0.734^X)$	$r^2 = 0.54$***
Time to flower (d)	Sigmoidal	$y = 51.3 * \exp(1.26 * 0.715^X)$	$r^2 = 0.58$***
Flowers (no.)	Linear	$y = 1.92 * x - 0.0195$	$r^2 = 0.65$***
Leaf length (cm)	-	-	N.S.
Leaf width (cm)	-	-	N.S.
SPAD	Linear	$y = 0.332 * x + 23.8$	$r^2 = 0.27$***
SLA (cm^2·g^{-1})	Linear	$y = -16.1 * x + 850$	$r^2 = 0.64$***
Stem length (cm)	Quadratic	$y = (-0.0180 * x^2) + (0.605 * x) + 18.0$	$r^2 = 0.07$***
Stem diameter (mm)	Linear	$y = 0.0631 * x + 3.02$	$r^2 = 0.25$***
Compactness (g·m^{-1})	Linear	$y = 0.967 * x + 1.12$	$r^2 = 0.84$***
SQ (cm·mm^{-1})	Linear	$y = -0.0790 * x + 6.98$	$r^2 = 0.13$***

the average DLI or eDLI was $\leq$ 10 and 13 mol·m^{-2}·d^{-1}, respectively, which is consistent with DLI values reported by Runkle and Blanchard (2011). In contrast, there was a linear response to (e)DLI for several growth parameters. For example, snapdragon grown under the clear-plastic and −FR2 treatments had the greatest number of open flowers and buds while those grown under the heavy shade had the fewest (~62% decrease) (Fig. 3, 4C).

Typically, it is desirable to produce floriculture crops as quickly as possible to minimize overhead costs and maximize the number of crop cycles grown in a year. Average DLI regulates time to flower (i.e., flower development rate) in a species- and cultivar-specific manner. For example, the maximum flower development rate saturates when the average DLI is between 6–12 mol·m^{-2}·d^{-1} for a large number of economically important bedding plants, although some saturate at a much higher DLI, for example, 20–25 mol·m^{-2}·d^{-1} for regal geranium (*Pelargonium* ×*domesticum* Baily) and hibiscus (*Hibiscus cisplatinus* St-Hil.) (Loehrlein and Craig 2004, Runkle and Blanchard 2011, Warner and Erwin 2003). Similar to other common bedding plants, snapdragon flower development rate saturated when the DLI was >10 mol·m^{-2}·d^{-1}, and in a previous agrivoltaics study on petunia, the saturation DLI was >7 mol·m^{-2}·d^{-1} (Stallknecht et al. 2023). Therefore, flowering of most (but not all) floriculture crops would likely not be delayed if PV panel transmission was ≥50% during the summer. However, during winter and early spring, such a decrease in (e)DLI would delay the flowering of some crops grown in temperate regions, necessitating PV panels that maximize light transmission and/or greater use of supplemental photosynthetic lighting.

Because most floriculture crops are judged primarily by their visual appearance, it is usually desirable to market plants with as many flowers and flower buds as possible. Similar to SDM, DLI influences the number of flowers produced by floriculture crops and varies within and between species. For instance, increasing the DLI to 15–20 mol·m^{-2}·d^{-1} increased the number of flowers of salvia (*Salvia splendens* Nees), impatiens, marigold (*Tegetes patula* L.), cyclamen, and snapdragon (Colantoni et al. 2018, Moccaldi and Runkle 2007, Oh et al. 2009, Pramuk and Runkle 2005, Warner and Erwin 2005). Snapdragon followed a similar trend and had the greatest flower number under a DLI of ~20 mol·m^{-2}·d^{-1}, and likely would have increased with higher DLI values since this response never saturated (Fig. 4C). In another study, experimental PV panels that provided ~20% shade (DLI estimated to be ~30 mol·m^{-2}·d^{-1}) did not decrease the number of flowers produced by petunia (*Petunia grandiflora* Juss.) and candytuft (*Iberis sempervirens* L.) during the summer in Italy (Colantoni et al. 2018). While an average DLI of 6–12 mol·m^{-2}·d^{-1} may not delay the flowering of many common bedding plants grown in the spring, this DLI range does not produce floriculture crops with the highest quality.

Morphology. Leaf length and width were not correlated to treatment (e)DLI (Table 3, 4). Relative chlorophyll content (SPAD) increased linearly with (e)DLI while individual leaf surface area (SLA) decreased linearly. Stem length was quadratically correlated to treatment (e)DLI but had a low r^2 value. Stem diameter increased linearly as (e)DLI increased. However, snapdragon stem diameter under the −R treatment was similarly narrow as that under the heavy-shade treatment but had a ~50% greater average (e)DLI (Table 1, 2). Thus, leaf length and width were affected by treatment spectra whereas SPAD, SLA, and stem diameter were primarily influenced by treatment (e)DLI. Similar to biomass accumulation, snapdragon tolerated a ~15% decrease in DLI and eDLI during the summer without significant changes to crop morphology.

Plants grown in low-light environments develop shade-avoidance and shade-acclimation responses such as greater stem elongation, increases in SLA, and a decrease in leaf chlorophyll concentration (Casal 2012). Increasing SLA (shade acclimation) and stem elongation (shade avoidance) can increase light interception and consequently increase RUE (Jayalath and van Iersel 2021). Snapdragon SLA and RUE were positively correlated under PV panel shading ($P<0.001$; $r^2=0.30$; data not shown). While SLA may not be a principal concern for snapdragon cultivation, floriculture crops grown for their foliage, such as coleus (*Coleus scutellarioides* L.), or food crops such as lettuce and basil, can be more susceptible to physical damage during production or harvest as SLA increases (Onoda et al. 2011). Many shade-avoidance and shade-acclimation responses are mediated through UV and B light-absorbing cryptochrome and R and FR light-absorbing phytochrome photoreceptors (Casal 2012, Meng et al. 2019, Park and Runkle 2018). Environments that create a phytochrome photoequilibrium (PPE) or internal phytochrome equilibrium (iPPE) <0.72 or <0.40, respectively (i.e., decreased R:FR) are indicative of plant canopy shading and the disproportionate absorption of B and R light relative to G and FR light. In this study, snapdragon stems were longer under the −R treatment (PPE=0.56, iPPE=0.25) than the moderate-shade treatment (PPE=0.69, iPPE=0.37) when the (e)DLI was similar. Therefore, consideration of (e)PAR transmittance and the light spectrum is needed when designing PV panels because of the possible effects on crop growth and morphology.

Floriculture crops grown in containers are commonly managed to have compact growth to facilitate shipping. Compactness (SDM per stem length) increased linearly with (e)DLI and was similar under the highest light transmission treatments (clear plastic, −NIR, −FR1, and −FR2) (Fig. 4D). As an additional quality consideration, potted floriculture crops such as snapdragon should remain upright during production, shipping, and sale. Snapdragon grown under the −R and heavy-shade treatments were more likely to fall over (lodging) than those in other treatments, and this occurred when the stem length to stem diameter ratio (i.e., SQ) was ≥5.5 cm·mm^{-1}. Similarly, some nursery tree species with a SQ >6 cm·mm^{-1} were prone to lodging, resulting in diminished crop quality or survivability after transplant (Jaenicke 1999). While SQ values related to lodging are likely species- and cultivar-specific, the SQ metric has not been reported in previous agrivoltaics studies and merits consideration in future studies with ornamental crops.

While metrics such as RUE or land equivalent ratio (LER) can be mathematically optimized for an agrivoltaic

system, both metrics ignore key quality parameters necessary for the marketability of floriculture crops (Toledo and Scognamiglio 2021). For instance, although snapdragon had the greatest RUE under the moderate- and heavy-shade treatments, flowering under those treatments was delayed, plants were less compact, and plants had fewer flowers. The LER most commonly compares the productivity of two monoculture agricultural systems to the productivity of an intercropped system (an agricultural system where more than one crop is grown simultaneously, and in the same area) and typically focuses on biomass accumulation. Similar to RUE, LER does not fully consider crop quality parameters, which are critical to ornamental crops. Furthermore, metrics such as LER often do not account for fluctuating commodity and energy prices with respect to time and the permanence of PV-greenhouse glazing materials. Consequently, agrivoltaic research that reports morphological attributes such as, but not limited to, compactness, SLA, branching, stem elongation, and flowering are needed to better characterize short- and long-term effects of PV materials on greenhouse crops.

In summary, snapdragon grown in the summer under simulated and experimental PV panels tolerated a decrease in average DLI and eDLI of around 15% (DLI and eDLI >17 and 19 $mol \cdot m^{-2} \cdot d^{-1}$, respectively) without significantly affecting biomass accumulation, compactness, number of flowers, or time to flower. This suggests floriculture production under PAR-transparent PV panels is possible when solar irradiance is high. In addition, semitransparent PV panels that absorbed (e)PAR, particularly red light, could have greater electricity generation than PAR-transparent PV panels, but at the expense of decreasing snapdragon crop quality. Despite having treatments with different transmitted light spectra, DLI or eDLI were similarly effective predictor variables for snapdragon growth and development. However, further research with additional species is needed to validate this conclusion. Given the economic importance of floriculture crops grown in greenhouses, additional agrivoltaic research on floriculture and other high-value specialty crops is needed to better understand trade-offs that can exist between electricity generation and various dimensions of plant quality.

Literature Cited

Amaducci, S., X. Yin, and M. Colauzzi. 2018. Agrivoltaic systems to optimize land use for electric energy production. Appl. Eng. 220:545–561.

Aroca-Delgado, R., J. Pérez-Alonso, Á.J. Callejón-Ferre, and M. Díaz-Pérez. 2019. Morphology, yield and quality of greenhouse tomato cultivation with flexible photovoltaic rooftop panels. Sci. Hortic. 257:108768.

Barron-Gafford, G.A., M.A. Pavao-Zuckerman, R.L. Minor, L.F. Sutter, I. Barnett-Moreno, D.T. Blackett, M. Thompson, K. Dimond, A.K. Gerlak, G.P. Nabhan, and J.E. Macknick. 2019. Agrivoltaics provide mutual benefits across the food–energy–water nexus in drylands. Nat. Sus. 2:848–855.

Both, A.J., 2002. Greenhouse glazing. Hort. Eng. Newsl. Rutgers Coop. Ext. 17:5–6.

Casal, J.J., 2012. Shade avoidance. The Arabidopsis book 10: e0157.

Colantoni, A., D. Monarca, A. Marucci, M. Cecchini, I. Zambon, F. Di Battista, D. Maccario, M.G. Saporito, and M. Beruto. 2018. Solar radiation distribution inside a greenhouse prototypal with photovoltaic mobile plant and effects on flower growth. Sustainability 10:855.

Cossu, M., A. Yano, S. Solinas, P.A. Deligios, M.T. Tiloca, A. Cossu, and L. Ledda. 2020. Agricultural sustainability estimation of the European photovoltaic greenhouses. Eur. J. Agron. 118:126074.

Dinesh, H. and J.M. Pearce. 2016. The potential of agrivoltaic systems. Renew. Sustain. Energy Rev. 54:299–308.

Faust, J.E. and J. Logan. 2018. Daily light integral: A research review and high-resolution maps of the United States. HortSci. 53:1250–1257.

Faust, J.E., V. Holcombe, N.C. Rajapakse, and D.R. Layne. 2005. The effect of daily light integral on bedding plant growth and flowering. HortSci. 40:645–649.

Giacomelli, G.A. and W.J. Roberts. 1993. Greenhouse covering systems. HortTech. 3:50–58.

Hassanien, R.H.E. and L. Ming. 2017. Influences of greenhouse-integrated semi-transparent photovoltaics on microclimate and lettuce growth. Int. J. Agri. Biol. Eng. 10:11–22.

Jaenicke, H. (1999) Good tree nursery practices: practical guidelines for research nurseries. Int. Cent. Res. Agroforestry 8–15.

Jayalath, T.C. and M.W. van Iersel. 2021. Canopy size and light use efficiency explain growth differences between lettuce and mizuna in vertical farms. Plants 10:704.

Kavga, A., I.F. Strati, V.J. Sinanoglou, C. Fotakis, G. Sotiroudis, P. Christodoulou, and P. Zoumpoulakis. 2019. Evaluating the experimental cultivation of peppers in low-energy-demand greenhouses. An interdisciplinary study. J. Sci. Food Ag. 99:781–789.

Ke, Xinglin, H. Yoshida, S. Hikosaka, and E. Goto. 2022. Optimization of photosynthetic photon flux density and light quality for increasing radiation-use efficiency in dwarf tomato under LED light at the vegetative growth stage. Plants 11:121.

Kusuma, P. and B. Bugbee. 2021. Improving the predictive value of phytochrome photoequilibrium: Consideration of spectral distortion within a leaf. Front. Plant Sci. 12:596943.

Loehrlein, M.M. and R. Craig. 2004. The effect of daily light integral on floral initiation of *Pelargonium* × *domesticum* LH Bailey. HortSci. 39:529–532.

Marcelis, L.F.M., A.G.M. Broekhuijsen, E. Meinen, E.M.F.M. Nijs, and M.G.M. Raaphorst. 2005. Quantification of the growth response to light quantity of greenhouse grown crops. Acta. Hortic. 711:97–104.

Marrou, H., J. Wéry, L. Dufour, and C. Dupraz. 2013. Productivity and radiation use efficiency of lettuces grown in the partial shade of photovoltaic panels. Eur. J. Agron. 44:54–66.

Meng, Q., J. Boldt, and E.S. Runkle. 2020. Blue radiation interacts with green radiation to influence growth and predominantly controls quality attributes of lettuce. J. Am. Soc. Hortic. Sci. 145:75–87.

Meng, Q., N. Kelly, and E.S. Runkle. 2019. Substituting green or far-red radiation for blue radiation induces shade avoidance and promotes growth in lettuce and kale. Environ. Exp. bot. 162:383–391.

Moccaldi, L.A. and E.S. Runkle. 2007. Modeling the effects of temperature and photosynthetic daily light integral on growth and flowering of *Salvia splendens* and *Tagetes patula*. J. Am. Soc. Hortic. Sci. 132:283–288.

Oh, W., I.H. Cheon, K.S. Kim, and E.S. Runkle. 2009. Photosynthetic daily light integral influences flowering time and crop characteristics of *Cyclamen persicum*. HortSci. 44:341–344.

Onoda, Y., M. Westoby, P.B. Adler, A.M. Choong, F.J. Clissold, J.H. Cornelissen, S. Díaz, N.J. Dominy, A. Elgart, L. Enrico, and P.V. Fine. 2011. Global patterns of leaf mechanical properties. Ecol. Lett. 14:301–312.

Park, Y. and E.S. Runkle. 2018. Far-red radiation and photosynthetic photon flux density independently regulate seedling growth but interactively regulate flowering. Environ. Exp. Bot. 155:206–216.

Pramuk, L.A. and E.S. Runkle. 2005. Modeling growth and development of Celosia and Impatiens in response to temperature and photosynthetic daily light integral. J. Am. Soc. Hortic. Sci. 130:813–818.

Proctor, K.W., G.S. Murthy, and C.W. Higgins. 2020. Agrivoltaics align with green new deal goals while supporting investment in the US' rural economy. Sustainability 13:137.

Runkle, E. and M. Blanchard. 2011. Saturating DLIs for flowering. Greenhouse Product News 21(2):42.

Stallknecht, E.J., C.K. Herrera, C. Yang, I. King, T.D. Sharkey, R.R. Lunt, and E.S. Runkle. 2023. Designing plant–transparent agrivoltaics. Sci. Rep. 13:1903.

Suddard-Bangsund, J., C.J. Traverse, M. Young, T.J. Patrick, Y. Zhao, and R.R. Lunt. 2016. Organic salts as a route to energy level control in low bandgap, high open-circuit voltage organic and transparent solar cells that approach the excitonic voltage limit. Adv. Energy Mater. 6:501659.

Tang, Y., X. Ma, M. Li, and Y. Wang. 2020. The effect of temperature and light on strawberry production in a solar greenhouse. Solar Energy 195:318–328.

Toledo, C. and A. Scognamiglio. 2021. Agrivoltaic systems design and assessment: a critical review, and a descriptive model towards a sustainable landscape vision (three-dimensional agrivoltaic patterns). Sustainability 13:6871.

Traverse, C.J., R. Pandey, M.C. Barr, and R.R. Lunt. 2017. Emergence of highly transparent photovoltaics for distributed applications. Nat. Energy 2:849–860.

USDA National Agricultural Statistics Service. 2022. Floriculture summary report. https://downloads.usda.library.cornell.edu/usda-esmis/files/0p0966899/s4656b62g/g445d913v/floran21.pdf. Accessed 2 Feb. 2023.

Von Elsner, B., D. Briassoulis, D. Waaijenberg, A. Mistriotis, Von Zabeltitz, C., Gratraud, J., Russo, G. and Suay-Cortes, R., 2000. Review of structural and functional characteristics of greenhouses in European Union countries: part I, design requirements. J. Ag. Eng. Res. 75:1–16.

Warner, R.M. and J.E. Erwin. 2003. Effect of photoperiod and daily light integral on flowering of five *Hibiscus* sp. Sci. Hortic. 97:341–351.

Warner, R.M. and J.E. Erwin. 2005. Prolonged high temperature exposure and daily light integral impact growth and flowering of five herbaceous ornamental species. J. Am. Soc. Hortic. Sci. 130:319–325.

Weselek, A., A. Ehmann, S. Zikeli, I. Lewandowski, S. Schindele, and P. Högy. 2019. Agrophotovoltaic systems: applications, challenges, and opportunities. A review. Agron. Sus. Dev. 39:1–20.

Wollaeger, H.M. and E.S. Runkle. 2014. Growth of impatiens, petunia, salvia, and tomato seedlings under blue, green, and red light-emitting diodes. HortSci. 49:734–740.

Zhen, S. and B. Bugbee. 2020. Far-red photons have equivalent efficiency to traditional photosynthetic photons: Implications for redefining photosynthetically active radiation. Plant Cell Environ. 43:1259–1272.